COMPOSITE MATERIAL PROPERTY NONDESTRUCTIVE CHARACTERIZATION USING OBLIQUELY INSONIFIED ULTRASONIC WAVES

Yoseph Bar-Cohen
JPL, California Institute of Technology
Pasadena, CA 91109

and

Ajit K. Mal and Shyh-Shiuh Lih
Mechanical, Aerospace, and Nuclear Engineering Department
University of California,
Los Angeles, CA 90024

To be submitted to SAMPE before 12-10-93

COMPOSITE MATERIAL PROPERTY NONDESTRUCTIVE CHARACTERIZATION USING OBLIQUELY INSONIFIED ULTRASONIC WAVES

Yoseph Bar-Cohen,
Jet Propulsion Laboratory, Caltech, Pasadena, CA 91109

Ajit K. Mal and Shyh-Shiuh Lih
MANE Dept, University of California, Los Angeles, CA 90024

ABSTRACT

The analysis of reflected ultrasonic waves induced by oblique insonification of composite materials is a powerful tool for providing information about defects and material properties. A device was developed to manipulate a pair of transmitting and receiving transducers at various angles of wave incidence and propagation with the fiber orientation. The device was designed as a C-scan attachment to allow inspection at specific locations as well as to obtain global information about the laminates by scanning them, Ultrasonic reflections from composite laminates are acquired and analyzed by a personal computer at high speed, in a transient or spectral form. Graphite/epoxy laminates were tested and the experimental results accurately corroborated the analysis of the wave behavior for tone-burst and pulse results. The inversion algorithm allows the determination of the material elastic constants as well as evaluation of various defects characteristics. The data repeatability and accuracy are very high, making oblique insonification methods easy to standardize for practical applications. This paper reviews the theoretical and experimental progress and examples of application to NDE of composites.

KEY WORDS: Non-Destructive Evaluation, Composites, Mechanical Properties.

INTRODUCTION

Fiber-reinforced composites are increasingly replacing metallic alloys as structural materials for primary components of fracture critical 'structures: This trend is the result of the

increasing understanding of the materials behavior and the recognition that composites have highly desirable properties that can be exploited to design structures with high performance characteristics. Composites have high stiffness, strength, fatigue resistance and damage tolerance and they are light weight. Further, they offer unique mix of formability and toughness allowing to imbed sensors and actuators in the material and to form active/adaptive (i.e., smart) structures.

However, composites are very sensitive to manufacturing processes and service conditions, which can induce defects and seriously degrade the material performance. In contrast to metals, the failure mechanisms of structural composites are much more complex and their ability to support loads can be affected significantly by factors to which metals are more tolerant. For example internal damage, caused by low –velocity foreign object impact or by rapidly applied localized thermal loads, can critically deteriorate the structure durability. Another major difficulty that hampers a wide use of composites is the lack of sufficient theoretical and experimental understanding of the material behavior at the micromechanical or fundamental level. This deficiency needs to be accounted for in the design allowable and it has led to the use of conservative safety margins. These safety margins are involved with weight penalties and they reduce the low-weight advantage of composites and increase the manufacturing cost in material and processing.

Nondestructive Evaluation (NDE) is a major factor in reducing the safety factors, assuring the conformance with design allowable and the performance specifications. NDE methods are needed to determine the structure integrity, stiffness, strength and durability (residual life). Since strength and durability are not physical parameters they cannot be measured by NDE means. On the other hand, the integrity and stiffness can be extracted directly from the NDE measurements. Specifically, NDE methods are developed to detect and characterize flaws and determine the material properties. Composites are multi-layered anisotropic media and therefore they were difficult to evaluate with conventional NDE methods which were originally developed to inspect isotropic materials. Testing composites has been a challenge to the NDE research community for many years and increasingly successful results are reported. Particularly., the use of oblique incident ultrasound is providing quantitative information about defects, adhesion, and the elastic properties [1-6].

Obliquely insonified ultrasonic waves are inducing various modes of wave propagation as well as inducing refractions and reflections, One of the phenomena that are the result of oblique isonification are the leaky Lamb waves (LLW). These waves were first observed in 1983 [7] when a Schlieren imaging system was used to examine the reflected field of ultrasonic waves at different frequencies. Subsequent studies by various researchers [2-6] modeled the phenomena and accurately correlated the results of the analysis. The behavior of LLW was tested for a wide range of composite materials including polymer matrix composites (PMC) such as graphite/epoxy, glass/epoxy and metal matrix composites (MMC), e.g., graphite/aluminum, graphite/copper and SiC/Ti.

A schematic diagram of the LLW phenomenon excitation for a plate immersed in fluid is shown in Figure 1. At frequencies that excite plate wave modes, LLW are induced when an ultrasonic wave is obliquely insonifies an immersed plate causing a distortion of the specular reflection (reflection from the composite as a half space). The specular reflection and the leaky wave interfere, a phase cancellation occurs and two components are generated with a null between them. The phenomena sensitivity to variations in boundary conditions, elastic properties, thickness and integrity provides detailed information about the material.

transversal y isotropic material, unidirectional fiber-reinforced composites are characterized by five independent effective stiffness constants. These constants dependent on the elastic properties of the fiber and matrix materials as well as their volume fraction,

Modeling the effective elastic moduli of composite materials has been the topic of many studies, Extensive discussions of the bounds for the effective elastic moduli of fiber-reinforced composites can be found in Christensen [9] and other associated literature cited therein. For low frequencies and low fiber concentration, the theoretical prediction of the effective elastic constants is in good agreement with experimental results [1 O]. On the other hand, for high frequencies the theoretical estimates are not satisfactory since the effect of wave scattering by the fibers becomes significant.

For fiber-reinforced composites, dissipation of the waves is caused by the viscoelastic nature of the resin and by multiple scattering from the fibers as well as other inhomogeneities. Both dissipation effects can be modeled by assuming complex and frequency-dependent stiffness constants, C_{ij} [6].

The interaction of ultrasonic wave, that obliquely insonifies a composite plate, leads to excitation of various elastic wave modes. These modes are strongly affected by the material integrity as well as the bulk and interface properties. The material characteristics can be extracted from the reflected and transmitted acoustic data that is acquired as a function of frequency and angle of incidence. A pitch-catch setup is assumed to be immersed in water insonifying a fiber-reinforced plate by a plane harmonic acoustic wave. To formulate the wave field a modified form of the potential function method described in Buchwald [11] is applied here.

For the formulation of the model, the displacement vector $\{u_1, u_2, u_3\}$ is expressed in terms of three scalar potentials $\Phi_j (j = 1, 2, 3)$ as follows

$$\begin{aligned} u_1 &= \partial\Phi_1/\partial x_1 \\ u_2 &= \partial\Phi_2/\partial x_2 + \partial\Phi_3/\partial x_3 \\ u_3 &= \partial\Phi_2/\partial x_3 - \partial\Phi_3/\partial x_2 \end{aligned} \quad (1)$$

Then the general solution of the Cauch y's equations of motion can be expressed

$$\begin{Bmatrix} \Phi_1 \\ \Phi_2 \\ \Phi_3 \end{Bmatrix} = \begin{bmatrix} q_{11} & q_{12} & 0 \\ q_{21} & q_{22} & 0 \\ 0 & 0 & 1 \end{bmatrix} \{ D \}\, e^{i(\xi_1 x_1 + \xi_2 x_2)} \quad (2)$$

where ξ_1, ξ_2 are the wavenumbers along the x_1 and x_2 directions, respective] y, and the vector { D } is in the form of

$$\{ D \} = Diag[\, e^{i\zeta_1 x_3}\ e^{i\zeta_2 x_3}\ e^{i\zeta_3 x_3}]\{C^+\} + Diag[\, e^{-i\zeta_1 x_3}\ e^{-i\zeta_2 x_3}\ e^{-i\zeta_3 x_3}]\{C^-\} \quad (3)$$

and the unknown vectors $\{C^+\} = \{C_1^+ C_2^+ C_3^+\}$ and {C-} = $\{C_1^- C_2^- C_3^-\}$. The "vertical" wavenumbers $\zeta_j (j = 1, 2, 3)$ and the factors q_{ij} (i, j = 1, 2) are dependent on the material symmetry. Then, the field equations incorporate the prescribed conditions at the two fluid-solid interfaces and the continuity conditions at the inner interfaces can be solved by a global matrix method suggested by Mal [13].

ELASTIC CONSTANTS INVERSION

Inversion of the elastic properties requires fitting the experiment data to the theoretical model where the stiffness matrix that is obtained represents the properties of the tested composite. A major difficulty in inverting the data is the need to solve a system of nonlinear equations, resulting in non-unique solutions. The authors applied a least square method for the nonlinear equations which is implicitly modeled by Britt and Luecke [14].

The minima in the amplitude spectra of the reflection coefficient R correspond to the modal frequencies of dispersive guided waves in the laminate. As shown earlier, the reflection coefficients are complex-valued functions of the frequency, laminate thickness and the material properties of both the composite and the surrounding fluid. Let R be expressed as

$$R = \Delta R + i\, AI \qquad (4)$$

where Δ_R is a smooth function. The modal frequencies of both free and leaky guided waves are almost identical in a broad frequency range. The real part of Eq. 4 is related to the dispersive guided waves and the imaginary part is contributed by the influence of water loading. Δ_I is approximately zero at the modal frequencies because of small influence of water loading, and dispersive guided waves are excited at frequencies at which Δ_R vanishes. The dispersive guided waves satisfy a system of equations that corresponds to the phase velocity or the angle of incidence in the form

$$A_R = G(f,\ C) \approx 0 \qquad (5)$$

where f is the vector of modal frequency and C is the vector of stiffness c_{ij}. The thickness of each lamina, mass densities of specimen and surrounding fluid as well as the acoustic wave speed are assumed to be constant. The objective of inversion is to find a set of maximum likelihood estimation of c_{ij} which satisfies Eq. 5. This requires minimization of the root-mean-square of the errors between the modal frequencies obtained from Eq. 5 and from the measured data. If the system of equations are linear, it could be directly solved and an exact solution may be obtained. Unfortunately, it is not possible to solve this inversion problem directly since Δ_R is a strong nonlinear function of the unknowns. An iterative procedure is necessary in seeking convergent solution of Eq. 5 until both $|f_{n+1} - f_n|$ and $|C_{n+1} - C_n|$ satisfy a convergence criterion.

In most recursive problems, the convergence speed of the solution is significantly affected by the initial guess. Deming's approximation [15] provides a convenient initial guess for the above interactive process. Further, the accuracy of the derivatives of the objective function has a strong influence on the convergence. For general multi-directional laminated composites, the derivatives of the reflection coefficient function is extremely complex, and it is difficult if not impossible to obtain exactly. A central difference method is used to approximate the first derivatives of G with respect to frequencies and material properties,

To determine the capability of the above reported inversion algorithm, the sensitivity of the dispersion curves to variations in the five elastic constants was examined [12]. Analysis of influence of variation of each of the five elastic constants have shown that only the constants c_{22}, c_{23} and C_{55} significantly affect the dispersion curves, whereas c_{11} leads to a small change at high phase velocities and c_{12} does not have any significant effect. Overall, C_{22}, c_{23} and C_{55} are the matrix dominated elastic constants and therefore they are the most sensitive to the

manufacturing (e.g. curing) process. Particularly, they are affected by the presence of porosity and variations in resin content. While the above three constants can be accurately inverted for uni-directional laminates, some degree of ill-posedness was observed when multi-orientation laminates were analyzed. For the later, the incorporation of the effect of the interracial epoxy layer between the various laminae added another degree of freedom to the analysis (For detailed discussion see [12]).

Time-domain experiments in certain directions offer an alternative method to determine the elastic constants c_{ij} accurately and efficiently. For the analysis, we are considering a unidirectional composite plate with thickness H and density ρ immersed in a fluid as shown in Figure 1 and the ray diagram is shown in Figure 2a. Here R" indicates the first reflected wave from the top surface of the plate, the rays labeled 1, 2, 3 are associated with the three transmitted waves inside the plate in a decreasing order of their speeds, the rays labeled 11, 12,...9 and 33 are associated with the waves reflected from the bottom of the plate, and T_1, T_2, T_3 indicate the waves transmitted into the fluid through the bottom of the plate. From Snell's law, the velocities V_k, V_l and the angles θ_k, θ_l are-related through

$$\frac{\sin\theta}{\alpha_0} = \frac{\sin\theta_k}{V_k} = \frac{\sin\theta_1}{V_1} \qquad (6)$$

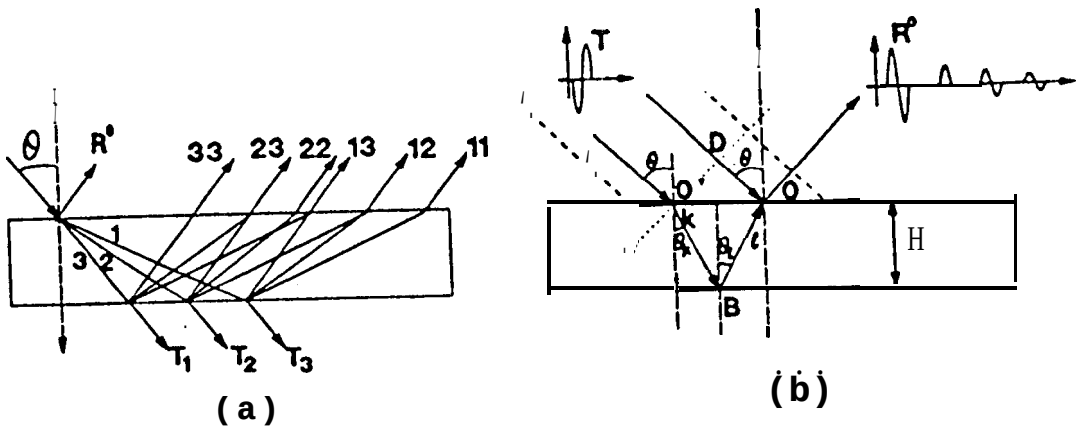

FIGURE 2. Ray diagrams of the reflected waves in a unidirectional composite laminate.

Two possible ray paths leading to the same point on the receiver are sketched in Figure 2b. If we denote the difference in the arrival times between rays along paths DO and O'BO by t_{kl}, then t_{kl} can be expressed as

$$t_{kl} = H(\zeta_k^* + \zeta_l^*) \qquad (7)$$

where $\zeta_k^* = \zeta_k/\omega$ is related to the elastic constants, and the details of the derivation of Eq. (7) can be found in [12] and is omitted here. The arrival time t_{kl} are related to the elastic constants c_{ij}'s, and thus these constant can be determined through the measured time-of-fight data. However, these relations are in germ-al nonlinear and do not lead to simple or unique solutions for the constants. As a result, small errors in the measurement of the arrival times may lead to large errors in the determined elastic constants.

It is known that there are three possible bulk wave speeds in a composite material and the wave speeds are functions of the propagation direction. Hence, for a fixed orientation ϕ to the fibers, the waves will become inhomogeneous or evanescent if the incident angle θ is larger than a certain critical incident angle θ_c. Similarly, for a fixed incident angle θ, the waves will become evanescent when the propagation angle ϕ is larger or smaller than a certain critical angle ϕ_c. By using these critical angle phenomena, the nonlinearity y in the inversion process can be avoided through appropriate choices of the incident angle θ and orientation ϕ as following experimental procedures.

a) *Pulse-echo experiment:* In this experiment only pure longitudinal waves are present. The travel time of the recorded pulse, t_{11} is related to the constant c_{22} through

$$c_{22} = 4\rho H^2 / t_{11}^2 \qquad (8)$$

Thus c_{22} can be determined from the pulse-echo experiment.

b) *Oblique insonification with ϕ = 90° and 0 less than the first critical incident θ_c:* Since the pulse associated with ζ_2 is not present in this case [12], the reflected signals arrive in the sequence "11" and "13". From the measured t_{11} and t_{13} the constant c_{23} can be determined from the relation

$$c_{23} = \frac{\rho}{(t_{11}/2H)^2 + \sin^2\theta/\alpha_0^2} - \frac{2\rho}{(t_{13}/H - t_{11}/2H)^2 + \sin^2\theta/\alpha_0^2} \qquad (9)$$

c) *Oblique insonification for a fixed incident angle θ:* After c_{22} and c_{23} have been determined, the constant c_{55} can be found as follows. With incident angle θ fixed, adjust ϕ such that the pulses "22" and "23" can be identified clearly. Then from measured t_{22} and t_{23}, c_{55} can be determined from

$$c_{55} = \frac{\rho\alpha_0^2}{\sin^2\theta\cos^2\phi}\left\{1 - \frac{(c_{22}-c_{23})}{2\rho}\left[\left(\frac{t_{23}}{H} - \frac{t_{22}}{2H}\right)^2 + \frac{\sin^2\theta\sin^2\phi}{\alpha_0^2}\right]\right\} \qquad (10)$$

d) *Oblique insonification with ϕ = 0° for θ smaller than the first critical θ_c:* The remaining two constants c_{11} and c_{12}, in principle, can be determined from the relations where t_{11} and t_{12}

$$c_{11} = \left[\frac{\alpha_0^2 c_{22} c_{55}}{\rho(c_{55}\sin^2\theta - \rho\alpha_0^2)\left(\frac{t_{11}}{2H}\right)^2}\left(\frac{t_{12}}{H} - \frac{t_{11}}{2H}\right)^2 + 1\right]\frac{\rho\alpha_0^2}{\sin^2\theta}$$

$$c_{12} = \left\{(c_{11}c_{22} + c_{55}^2) - \frac{\alpha_0^2}{\sin^2\theta}\left[\rho(c_{22}+c_{55}) - c_{11}c_{55}\left(\left(\frac{t_{11}}{2H}\right)^2 + \left(\frac{t_{12}}{H} - \frac{t_{11}}{2H}\right)^2\right)\right]\right. \qquad (11)$$

are the arrival times of the first two (11 and 12) pulses. However, it is difficult to measure t_{11} and t_{12} in the present setup due to the geometry limitation of available transducers. To clearly identify pulses 11 and 12, an incident angle smaller than the first critical θ_c associated with ζ_1 is required. For unidirectional graphite/epoxy laminate, the first critical angle θ_c for $\phi = 0°$ is approximately equal to 8.4° and this angle is difficult to achieve because the transducers will contact each other in such a small angle. Our calculations have shown that

for a given incident angle θ, the reflected field changes significantly near the critical angle ϕ_c. The arrival times of these pulses are strongly affected by c_{11} near critical angles. We use this critical angle phenomenon to determine the constants C_{11} and C_{12}.

Recall that the equation for the bulk wave speed V can be written as

$$[(a_1 - a_5) + (a_5 - V^2)^2/n_2^2]\, a_2 - a_3^2 = -[(a_5 - V^2)^2 + (a_5 - V^2)(-a_5 + a_1 n_2^2) + a_5(a_1 - a_5) n_1^2 n_2^2]/n_1^2 n_2^2 \quad (12)$$

where $n_1 = \cos\phi$, $n_2 = \sin\phi$. Where

$$a_1 = c_{22}/\rho,\ a_2 = c_{11}/\rho,\ a_3 = (c_{12} + c_{55})/\rho,\ a_4 = (c_{22} - c_{23})/2\rho,\ a_5 = \quad (13)$$

The remaining unknowns c_{11} and c_{12} can then be calculated from two measured critical angles ϕ_c with $V = \alpha_o/\sin\theta$ at two different incident angles θ.

EXPERIMENT

A unique experimental setup (see Figure 1) was designed to perform the various oblique insonification configurations that are needed to corroborate the theory and to practically implement the results [12]. The setup was mounted as an attachment to a computer control C-scan (made by AIT) and can be used to perform LLW, pulse-echo and polar-backscattering tests for evaluation of both defects and elastic constants [8]. The setup controls the polar and incidence angles of the transducers as well as the excitation frequency and can be articulated to position the receiver at the null zone. The transducer pair is controlled in a pitch-catch configuration orienting the incidence angles from 12 to 75 degrees with minimum increment of 0.05 degrees. Further, the setup can vary the polar angle from O to 360 degrees with increments of .1 degrees. The height of the setup can be controlled within a range of 4.0 inches in increments of 0.5 roil.

Tone-burst signals with a duration sufficiently long to establish a steady-state condition in the test specimen, are produced by an HP 8116A Signal Generator. This device can produce tone-burst signals with a frequency up to 40 Mhz and it can perform frequency sweep up to 50 MHz. The received signals are amplified by the broadband amplifier component of a Panametrics 5052UA pulser/receiver. This pulser/receiver is also used as a broadband transmitter for excitation of short duration pulses. The received signals are converted from radio frequency (RF) display to video after further amplification using a broadband receiver Matec Model 615. For tone-burst tests, only the steady state region is analyzed by gaging it with a Stanford Research Boxcar Gated Averager Model SR250. To select the transmitted frequency and to acquire the data a 486/50 MHz personal computer is used with an IEEE-488 interface. To examine pulses in the time-domain, signals from the pulser/receiver are digitized with a LeCroy 9410 Digital Dual 150 MHz Oscilloscope prior to acquisition by the computer.

A computer code was written to control the incidence and polar angles, the height of the transducers from the sample surface and the transmitted frequency. Signals (tune-burst or

Using a combination of LLW setup and a C-scan system [8], defects such as delamination, porosity, ply gaps, matrix cracking and resin content variations were easily detected. Each type of these defects is characterized by a unique spectral response enabling the identification of the defect type. LLW sensitivity to variations in interface characteristics allows evaluation of bonded joints [1]. Moreover, through data inversion the material elastic constants can be

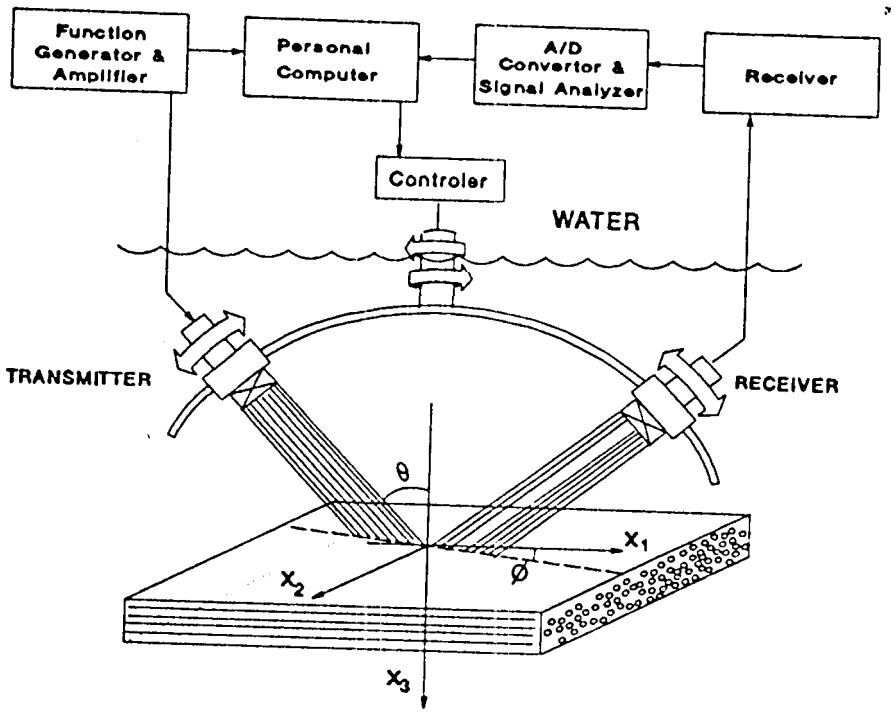

FIGURE 1. The experimental set-up and schematic description of the leaky Lamb wave phenomenon.

determined [12] and used to estimate the volume content of resin as well as porosity content [3]. This paper reviews the recent theoretical and experimental progress that the authors made towards implementing oblique insonification methods for NDE of composite materials. The emphasis of this paper is on Graphite/Epoxy unidirectional laminates.

WAVE PROPAGATION MODELING

The behavior of an ultrasonic wave propagating through a composite material is determined by the stiffness matrix and the wave attenuation. To determine this behavior several assumptions can be made about fiber reinforced composite materials. The material can be treated as homogeneous since the fiber diameter (e. g., graphite 5-10pm and glass 10-15μ) is significantly smaller than the wavelength (for frequencies up to 20 Mhz the wavelength is larger than 100μ). Each layer is assumed transversely isotropic bonded with a thin layer of an isotropic resin. The mechanical behavior of an individual lamina is described by an average of the displacements, the stresses and the strains over representative elements. The average strains are related to the average stresses through the effective elastic moduli. As a

pulses) are acquired as a function of the polar and incidence angles and are saved in a file for corroboration with the theoretical predictions. Tone bursts are used to determine the LLW modes and to prepare dispersion curves (phase velocity as a function of frequency). The frequency is varied within the transducer response range (up to 20dB below the maximum amplitude) and the modes are identified for each angle of incidence from 12 to 50 degrees to allow the use of free-plate theoretical calculations. Incrementally, the incident angle is changed within the selected range and the reflection spectra acquired. At each given incidence angle, the minima are identified and are added to the accumulating dispersion that is plotted simultaneously on the computer display (Figure 3). The currently acquired minima are uniquely identified on both the spectra and the dispersion curve while the data acquisition is in progress. For a test along the 0° polar angle (along the fiber direction), Figure 3a is showing the reflection spectra for an arbitrary incidence angle. Whereas, Figure 3b shows the accumulating dispersion curve.

For each tested composite, dispersion curves were prepared for three separate planes (0°, 45°, and 90°) where the angle of incidence is converted to a phase velocity through Snell's law. An example of the theoretical vs. experimental dispersion curves for a $[0]_8$ Gr/Ep

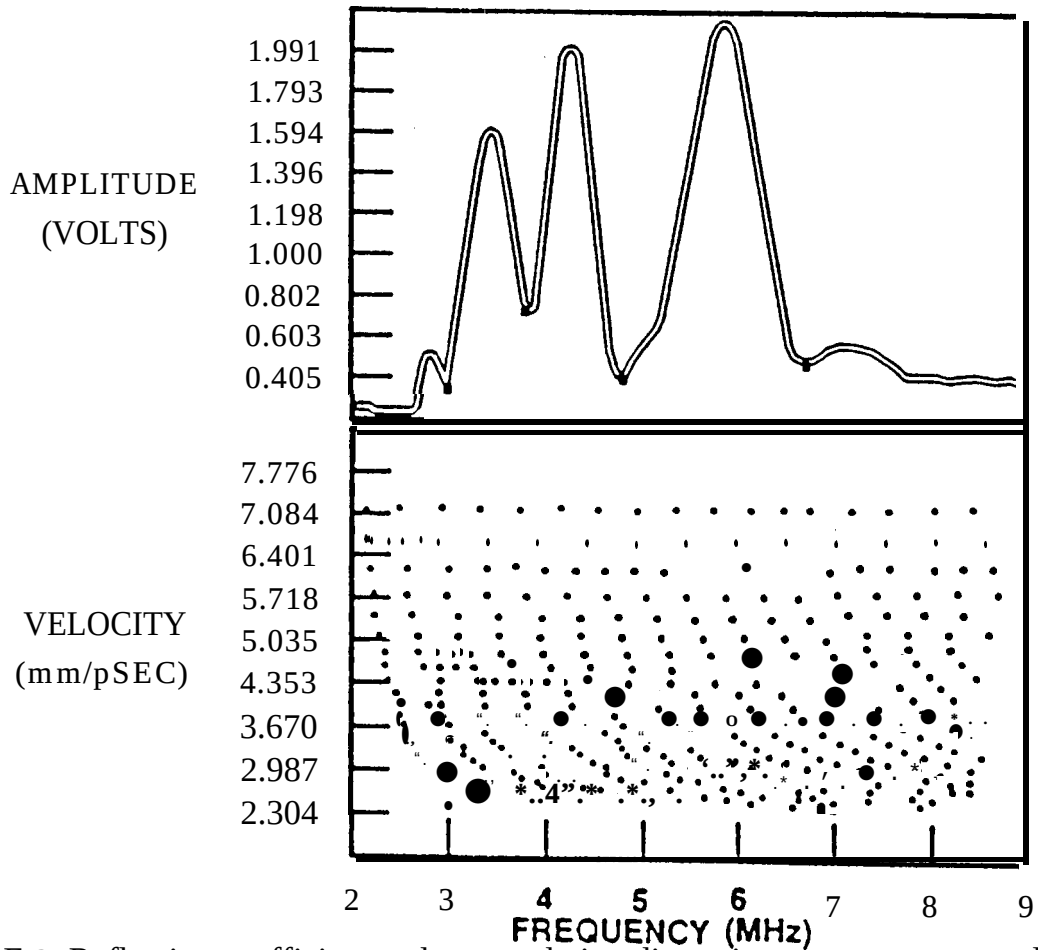

FIGURE 3. Reflection coefficient and accumulating dispersion curve as presented simultaneously during data acquisition.

AS4/3501-6 laminate is shown in Figure 4. Only minima that are associated with more than 4 percent drop in amplitude were recorded. This approach reduces the possibility of acquiring noise as data. Since transducers have a limited frequency range, dispersion curves arc established by using 0.5-, 1-, 2.25-, 5- and 1O-MHZ transducer pairs. For each pair, a

frequency sweep is conducted within the range of the transducer response up to the frequencies where the amplitude drops 10 db below the maximum for the particular reflection spectra. In Figure 4 the dispersion curve covers the frequency range from ,1 to 18 MHz and along the fiber orientation 11 mode are clearly identified. A careful review of Figure 4 shows an overlap of subsequent spectra of different transducers which is showing the high degree of accuracy.

RESULTS

Polymer and metal matrix composites were tested to determine the capability of ultrasonic oblique insonification methods as means
of detecting defects and inverting material properties. Using
the LLW inversion algorithm and the experimental setup described earlier, the elastic properties *were* determined for a 3.378 mm thick graphite/epoxy AS4/350 1-6 laminates. The properties for an 24-layer unidirectional laminate are give in Table 1.

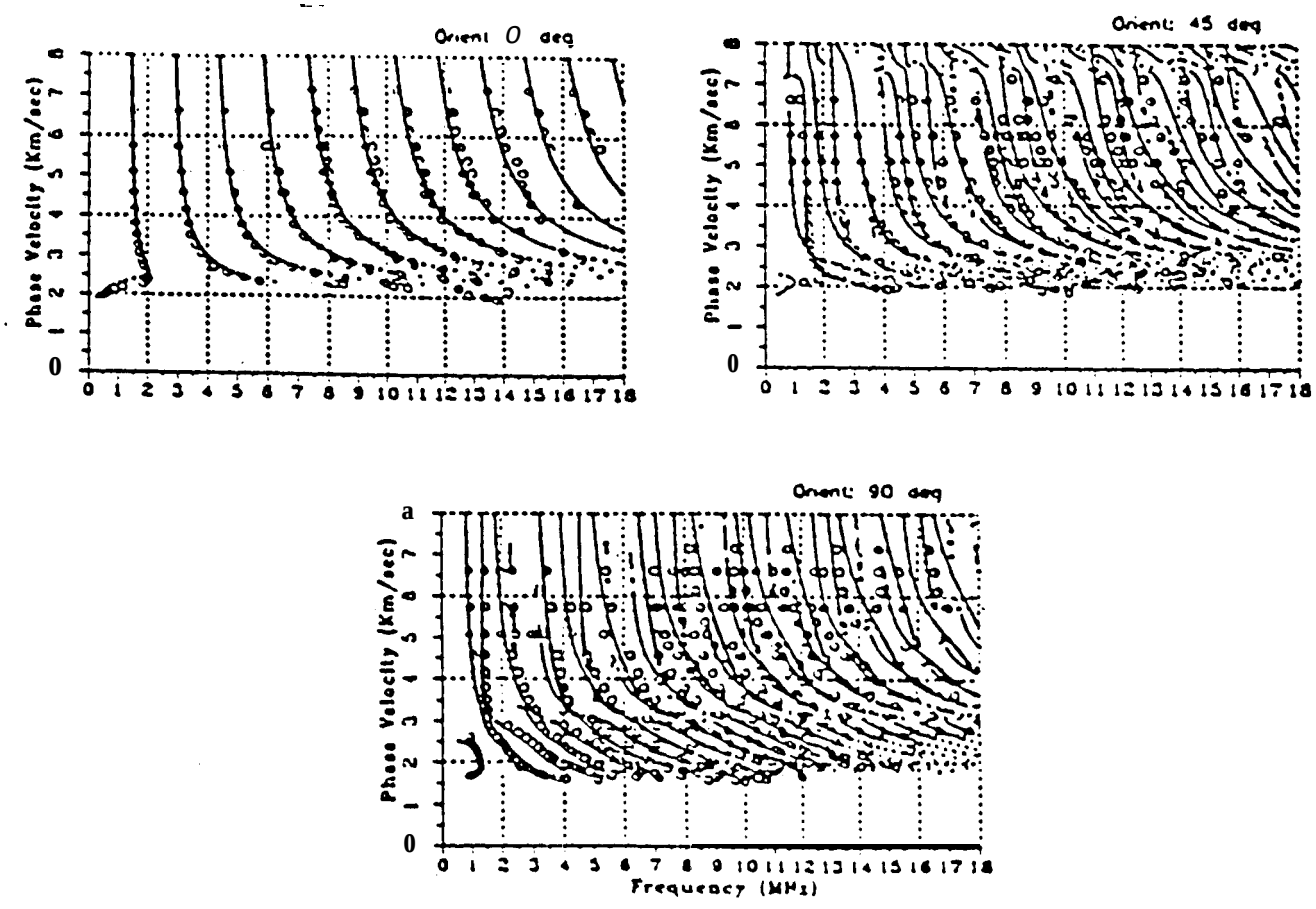

FIGURE 4, Dispersion curves for unidirectional laminate along 0°, 45° and 90" with the fiber orientation.

Theoretical and experimental dispersion curves were compared for a 1 mm thick 8 layers. graphite/epoxy AS4/3501 -6 laminates with unidirectional, cross-pi y and quasi-isotropic layups. The results of the model were corroborated with an excellent agreement. Figures 4

are showing the results for the unidirectional laminate tested at 0°, 45° and 90° propagation angle with the fibers of the first layer. Tests were also made on thick composite laminates and specifically a 25 mm thick $[0]_{176}$ layup. To overcome the deficiency of the LLW method in determining the fiber dominated elastic constant, time-domain experimental data and the analysis obtained from ray theory were used.

TABLE 1: Inverted stiffness constants for graphite/epoxy AS4/3501-6 $[0]_{24}$ laminate.

ρ (g/cm*)	c_{11} (GPa)	c_{12} (GPa)	c_{22} (GPa)	c_{23} (GPa)	c_{55} (GPa)
1.578	166.07	7.09	16.19	7.52	7.79

The time histones of the reflected signal for a unidirectional 3.378 mm thick AS4/3501-6 graphite/epoxy composite are shown in figure 5 for different incident angles and directions.

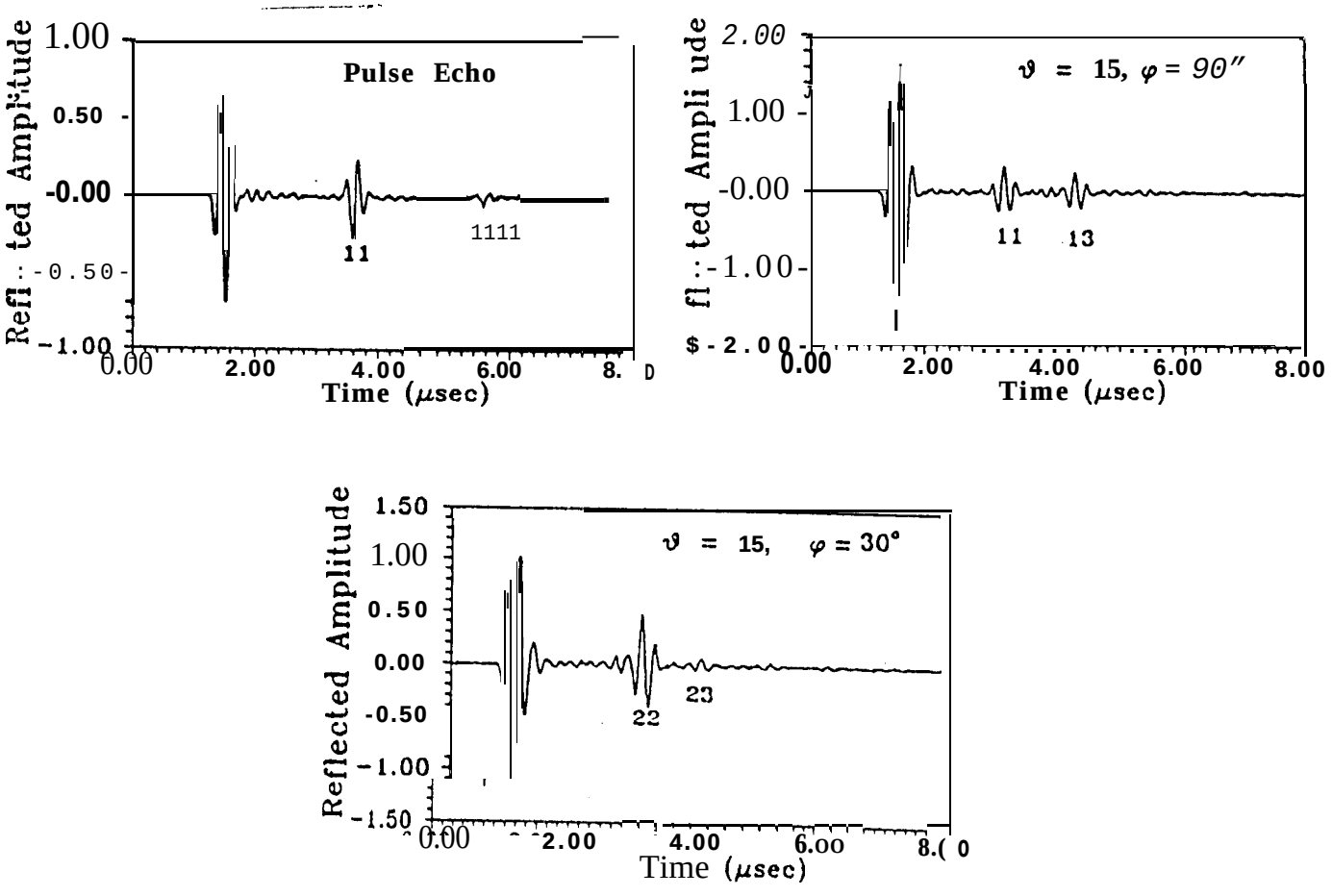

FIGURE 5. Reflected signal from a 3.378 mm thick composite for: a. pulse-echo mode, b. e = 15° & ϕ = 90° and c. θ = 15° & ϕ = 30°.

The pulse-echo data is shown in Fig. 5a, where $t_{11} \approx 2.10$ μsec and c_{22} is found from Eq. 8 to be 16.3 GPa. For incidence at θ = 15° an ϕ = 90° the reflected signal is shown in Fig. 5b, $t_{11} \approx 1.74$ μsec and t_{13} = 2.86 μsec, and c_{23} can be calculated from Eq. 10 as 7.95 GPa.

Similarly, for $\theta = 15°$ and $\phi = 30°$ (Fig. 5c), $t_{22} \approx 2.03$ μsec and $t_{23} \approx 2.95$ μsec, from which C_{55} can be determined from Eq. 10 as 7.74 GPa. Two critical cases were measured as $\phi_c = 58.1°$ for $\theta = 15°$, and $\phi_c = 68.7°$ for $\theta = 20°$. These two cases are used to calculate c_{11} and c_{12} from Eq. 12 as 162.09 and 6.71 GPa, respectively. The inverted elastic constants are listed in Table 1. A detailed description of the procedure and the error analysis can be found in [6] and are omitted here. Detailed description of the procedure and the error analysis can be found in [12].

To produce an image of inherent defects, C-scans were prepared using the LLW setup and pulses as well as tone-bursts. Pulses provided much more effective defects imaging capability than using a single LLW mode in tone-burst. C-scan images were made using pulses where the variables that were examined included the time-of-flight and amplitude. All three types of embedded defects - delamination, porosity and ply-gap were clearly identified [8].

DISCUSSION

Theoretical and experimental studies of oblique insonification of composite materials have shown excellent results for uni-directional graphite/epoxy composite. The need for an access from one side to the test laminate make these methods effective for practical applications. The LLW scanner, that was developed by the authors, provides a high speed data acquisition system for the determination of dispersion curves. This device also can be used to acquire pulse data and to optimize the test parameters for a C-scan imaging. The important features of the reflected signals in oblique incidence experiments, including the LLW method, were clearly explained through a generalized ray theory. The analysis presented here shows that the overall reflected signal is the result of small number of rays. The irregular behavior of the reflected field is caused by mode-converted waves, many of which are attenuated during the reflection. For waves propagating in the plane parallel or perpendicular to the fibers, the reflected acoustic field from the fiber-reinforced composite is similar to that of the isotropic case in many aspects. However, there are significant differences in certain properties of the field even for propagation perpendicular to the fibers,

Inclusion of material dissipation in the theoretical simulation of the LLW experiment improved the accuracy of predicting the wave amplitude, especially at higher fH values. The phenomenological model of wave attenuation presented here yielded results that are in excellent agreement with the laboratory measurements. When compared to LLW data for a relatively thick, unidirectional composite plate, the exact solution for the elastodynamic problem predicts a large number of minima in reflected amplitude spectra. The analysis shows that these minima in the LLW spectra are caused by the interference of bulk waves rather than the appearance of guided waves in the plate.

The success of the modeling has led to an ability to invert accurately all constants of a unidirectional graphite/epoxy laminate. To apply this model to other types of composite layups and materials, there is a need for further studies to evaluate the applicability of the model. It is well known that the stiffness constants c_{22}, c_{23} and c_{55} of the unidirectional composite have a strong influence on the dispersion curves of both leaky and free Lamb waves. Hence, these three constants are determined accurately through appropriate inversion schemes of the LLW data, Due to their weak influence on the dispersion curves, the other two material constants c_{11} and c_{12} must be determined through measurement of critical angles

using pulsed oblique incidence ultrasonics and time-of-flight measurements. Pulse-Echo is used to determine c_{22} which can also be confirmed by tests at an oblique incidence along the 90° orientation to the fibers. Measurements at this orientation can also be used to determine c_{23}. Tests at off-axis orientations, ϕ, that are below the critical orientation, ϕ_c, can be used to determine the third matrix dominated constant c_{55}. Using two oblique incidence angles along the fiber orientation one can determine c_{11} and c_{12} with a very high sensitivity to experimental variations. On the other hand, the same tests performed along the critical propagation orientation, ϕ_c, for the given incidence angle, θ, leads to significantly more accurate inversion of these constants.

Imaging defects using C-scan system combined with an oblique insonification were very successful when unidirectional laminates were tested. Defects such as delamination, porosity and ply-gaps were easily detected. Generally, the acceptance/rejection criteria are well established in a wide range of industry and standards which can be easily applied for angular insonification tests. Porosity rejection criteria, on the other hand, are

widely based on volume fraction data where, in most cases, porosity volume fraction below two percent is acceptable. Unfortunately, there is no NDE method which can accurately and reliably determine the volume fraction of porosity. The results using oblique insonification are indicated offer a new form of porosity characterization. Generally, it is easier to relate to a single parameter that identify porosity, namely volume fraction. However, this parameter does not provide sufficient information to determine the effect on the performance of a structure. Porosity with the same volume fraction but with different characteristic size, location and distribution will have different effect on the mechanical behavior of the laminate. These characteristic parameters can be extracted from oblique incidence C-scan data. Therefore, relevant accept/reject criteria are needed to define limits for the various characteristics of porosity.

ACKNOWLEDGEMENT

This research was supported by the AFOSR under grant F49620-93- 1-0320 monitored by Dr. Walter Jones. The part of the study that was carried out at the Jet Propulsion Laboratory (JPL), California Institute of Technology (Cal tech), was performed under a contract with the NASA.

REFERENCES

1. A. K. Ma], P. -C. Xu, and Y. Bar-Cohen, "Leaky Lamb Waves for the Ultrasonic Nondestructive Evaluation of Adhesive Bonds, " Journal of Engineering Materials and Technology Transaction of ASME, Vol. 112, No. 3, (1990), pp. 255-259.

2. V. Dayal and V. K, Kinra, "Leaky Lamb Waves in an Anisotropic Plate. 11: Nondestructive Evaluation of Matrix cracks in Fiber-Reinforced Composites," J. Acoustic Society of America, Vol. 89, No. 4 (1991), pp. 1590-1598.

3. K. Balasubramanian and J. Rose, "Physically Based Dispersion Curve Feature Analysis in the NDE of Composite Material s," Research in Nondestructive Evaluation, Vol. 3, No, 1 (1991) pp. 41-67.

4. A. H. Nayfeh and D. E. Chimenti, "Ultrasonic Wave Reflection from Liquid-Loaded Orthotropic Plates with Applications to Fibrous Composites, " J. Applied Mechanics, Vol. 55 (1988) p. 863.

5. D. P. Jansen and D. A. Hutchins, "Lamb wave immersion Topography, " Ultrasonics, Vol. 30 (1992) pp. 245-254.

6. A. K. Mal and Y. Bar-Cohen, "Ultrasonic Characterization of Composite Laminates, " Wave Propagation in Structural Composites, Proceedings of the Joint ASME and SE meeting, AMD-Vol. 90, A. K. Mal and T. C. T. Ting (Eds.), ASME, NY, (1988), pp. 1-16.

7. Y. Bar-Cohen and D. E. Chimenti, "Leaky Lamb Waves in Fiber-Reinforced Composite Plates," Review of Progress in QNDE, Vol. 3B, D. O. Thompson and D. E. Chimenti (Eds.), Plenum Press, New York and London (1984), pp. 1043-1049.

8. Y. Bar-Cohen and A. K. Mal, "Characterization of Composite Laminates Using Combined LLW and PBS Methods," Review of Progress in QNDE, Vol. 10B, D.O. Thompson and D.E. Chimenti (Eds.), Plenum Press, New York, (1991) pp. 1555-1560.

9. R. M. Christensen, "Mechanics of Composite Materials, " Chapter 4, Wiley, New York (1981).

10. S. K. Bose and A. K. Mal, "Longitudinal Shear Waves in a Fiber-Reinforced Composite, " International J. of Solid Structures, Vol. 9, (1973) pp. 1075-1085.

11. V. T. Buchwald, "Rayleigh Waves in Transversely Isotropic Media, " Quarterly J. Mechanics and Applied Mathematics, Vol. 14 (1961) pp. 293-317.

12. A. K. Mal, S. -S. Lib, and Y. Bar-Cohen, "Nondestructive Characterization of the Elastic Constants of Fiber Reinforced Composite, " Proceedings of the 34th AIAA/ASME/ASCE/AHS/ASC Structures, Structural Dynamics and Materials Conference, Part 1, AIAA-93-1394-CP, Held in La Jolla, CA April 19-22, 1993, pp. 472-484.

13. A. K.' Mal, "Wave Propagation in Layered Composite Laminates Under Periodic Surface Loads. " Wave Motion, Vol. 10, (1988), PP. 257-166.

14. H. I. Britt and R. H. Lueche, "The Estimation of Parameters in nonlinear, Implicit Models, " Technometrics, Vol. 15 (1973) pp. 233-247.

15, W. E. Demig, "Statistical Adjustment of Data, " Wiley, New York, (1943).